Basic mechanisms of structural relaxation and diffusion in amorphous silicon

G. T. Barkema[1], Normand Mousseau[2†], R.L.C. Vink[3] and Parthapratim Biswas[4]
(1) Theoretical Physics, Utrecht University, Utrecht, The Netherlands
(2) Department of Physics and Astronomy and CMSS, Ohio University, Athens, OH 45701, USA
(3) Institute Fysische Informatica, Utrecht University, Utrecht, The Netherlands
(4) Debye Institute, Utrecht University, Utrecht, The Netherlands

ABSTRACT

The low-temperature dynamics in amorphous silicon occurs through a sequence of discrete, activated events that reorganize the topology of the network. In this review, we present some recent work done to understand better the nature of these events and the associated dynamics in *a*-Si. Using the activation-relaxation technique (ART), we generated more than 8000 events in a 1000-atom model of *a*-Si, providing an extensive database of relaxation and diffusion mechanisms. The generic properties of these events, such as the number of involved atoms and the activation energies, were investigated and found to be in agreement with experimental data. As it turns out, the bond-transposition mechanism proposed by Wooten, Winer and Weaire (WWW) some time ago plays an important role in the events generated by ART. We have therefore turned to an optimized version of the WWW algorithm to generate the best overall configurations of *a*-Si available today. We discuss the details of the optimization and present the structural and electornic properties of the resulting models.

INTRODUCTION

At temperatures well below melting, the microscopic evolution of materials occurs through a sequence of activated processes, in which the energy barriers crossed are high compared to the average thermal energy. The high degree of symmetry characterizing crystalline materials implies that only a small set of atomistic mechanisms are responsible for the activated dynamics. The situation is completely different in disordered materials: as a consequence of the lack of symmetry, the nature of the activated mechanisms varies as a function of the local environment. The standard approach to study these microscopic mechanisms, introduced by Weber and Stillinger [1], is to simulate a material at a high temperature and to quench configurations at regular intervals. At a sufficiently high temperature, and sufficiently long time intervals, the quenches will result in distinct configurations, and their sequence may provide a basis for the reconstruction of activated dynamics. Difficulties arise, however, since (1) it is unclear whether the reconstructed path is the one that the configuration would follow if simulated at lower temperature and (2) the prefactor of the diffusion constant often favors different mechanisms at high and low temperatures [2].

A different avenue to explore microscopic mechanisms is provided by the activation-relaxation technique [3, 4, 5]. In the first part of this manuscript we review the results obtained with this method for the study of amorphous silicon (*a*-Si).

Applying the activation-relaxation technique to *a*-Si, we find that the microscopic dynamics is dominated by a combination of one or more *bond transpositions*. This mechanism was already

†Present address: Département de physique, Université de Montréal, C.P. 6128 succ. Centre-ville, Montréal (Québec), Canada H3T 1T7; e-mail: mousseau@physcn.umontreal.ca.

proposed by Wooten, Winer and Weaire [6, 7] as the basis for an algorithm for the generation of continuous random network (CRN) structures. It appears now that this mechanism could also be the one favored by nature.

This gives us a justification to go back to the original ideas of the *sillium* approach of Wooten, Winer and Weaire [6, 7] for the preparation of models of amorphous silicon. The second part of this manuscript reviews in details the several algorithmic improvements we made to the original *sillium* algorithm, resulting in an efficiency gain of a few orders of magnitude.

We then continue with a discussion of the structural and electronic properties of the atomic configurations generated with this improved algorithm. Furthermore, an outlook to future research is presented.

MICROSCOPIC MECHANISMS IN AMORPHOUS SILICON

In experimental studies, Frank *et al.* have measured the activation energy for self-diffusion in crystalline silicon to be 4.5 ± 0.5 eV [8]. The situation is not as clear for *a*–Si, since its properties depend closely on the preparation method and the annealing schedule of the samples. It is therefore not surprising that the activation energy of self-diffusion reported for this material shows a wide range of values, suggesting a multiplicity of mechanisms. In differential calorimetric and conductivity measurements on samples freshly prepared by ion-bombardment, the average activation barrier is found to vary from 0.23 to 2.70 eV, depending on the degree of structural relaxation and temperature [9, 10]. Since samples are far from equilibrium, these barriers are lower bounds: barriers are likely to be higher in well relaxed samples, possibily reaching values similar to that found in crystalline silicon.

There is also controversy regarding the nature of relaxation and diffusion mechanisms: calorimetric and Raman measurements indicate that relaxation should be local, involving relaxation of point defects [9], while Mössbauer experiments suggest that up to 10^4 atoms are involved, at least to some degree, in the relaxation of a single dangling bond [11].

We recently addressed the nature of structural relaxation and diffusion in *a*-Si numerically using the activation-relaxation technique (ART) [3, 4, 5]. Starting from a series of independent, well-relaxed configurations prepared with ART, we generated, also with ART, a database of more than 8000 activated events (involving structural changes in the topological bond network). The probability of occurence of events in the database depends on the biases of ART and cannot be given, at this moment, a physical meaning; there is numerical evidence that these biases are Boltzmann-like [12] but a rigorous proof is still missing. As a result, it is unclear if the frequency of events occurring in an ART simulation is the same as it would occur in nature. In order to verify the quality of the events, 800 events were re-analysed using the nudged-elastic-band method [13, 14], which reconstructs the minimum-energy path between two local energy minima. It was found that, for the majority, events found with ART correspond to real activated mechanisms within the limits of our interaction potential although the exact height of the barrier can be off by up to 1 eV in either direction [15].

In spite of these limitations, it is still instructive to study the energetics of the events occurring in the database. For each event, we calculate the energy asymmetry (the energy difference between the initial and final configurations) and the energy barrier (the difference between the saddle point and the initial configuration). A histogram of both quantities is shown in Fig. 1 for the whole set of 8000 events.

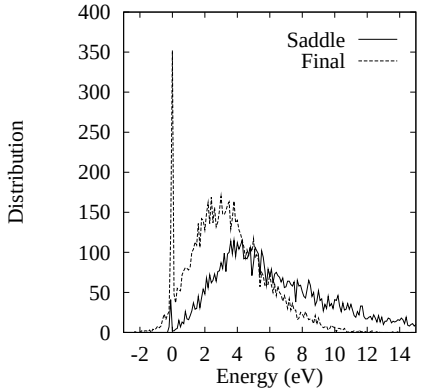

Figure 1: Distribution of the energy barrier (solid) and the energy asymmetry (dashed) for 8106 ART generated events.

Fig. 1 shows a continuous distribution of the energy barrier which is in agreement with experimental data [9]. The distribution for the energy barrier peaks at around 4 eV and tails off beyond 15 eV. From the path-reconstruction, it was found that most high-energy-barrier events break up into multiple sub-events, leading to an overall decrease in the energy of at the peak of the distribution by as much as 1.5 eV [15]. Most activated mechanisms lead to states of higher energy, as is to be expected since we start from a well-relaxed state. Two more striking features are the small peak around 0 eV in the distribution of the energy barrier and the large peak in the distribution of the energy asymmetry. The first is associated with unstable configurations, the latter corresponds to atomic exchanges as discussed below.

In Fig. 2a, we plot a histogram of the square root of the sum of the squared atomic displacements; this corresponds to the euclidean distance (in $3N$-dimensional phase space) between the initial and final configuration. The histogram peaks at around 2.75 Å, slightly more than one atomic distance, with a spread of about 1 Å. The number of atoms that contribute significantly to this distance, defined as those that are displaced by more than a distance r_c, is plotted as a function of r_c in Fig. 2b.

Finally, we investigate the change in topology that occurs during the events. The topology of the network is defined by the bonds between the atoms. Here, two atoms are bonded when their separation is less than 3.0 Å, a value obtained from the radial distribution function (RDF) of *a*-Si [16]. We limit our study to those events involving directly four-fold coordinated atoms only. The database contains 802 of these events.

Three mechanisms account for more than 85% of the events. The most frequent type of event, with 68%, is one in which two bond-sharing atoms exchange a pair of neighbors. This event is illustrated in Fig. 3a. It corresponds, unexpectedly, to the bond-switching algorithm of Wooten, Winer and Weaire [6, 7]. These events display a narrow range of activation energies centered around 2 eV. The second most common type of event, illustrated in Fig. 3b, accounts for 12% of all events. It involves perfect switches of two nearest-neighbor atoms. This mechanism, called concerted-exchange (CE), was proposed by Pandey to explain self-diffusion in *c*-Si [17]. The activation energies for such CE events range from 3.6 eV to about 12 eV; clearly bond transpositions are energetically more favorable. The CE event can be regarded as a combination of three bond

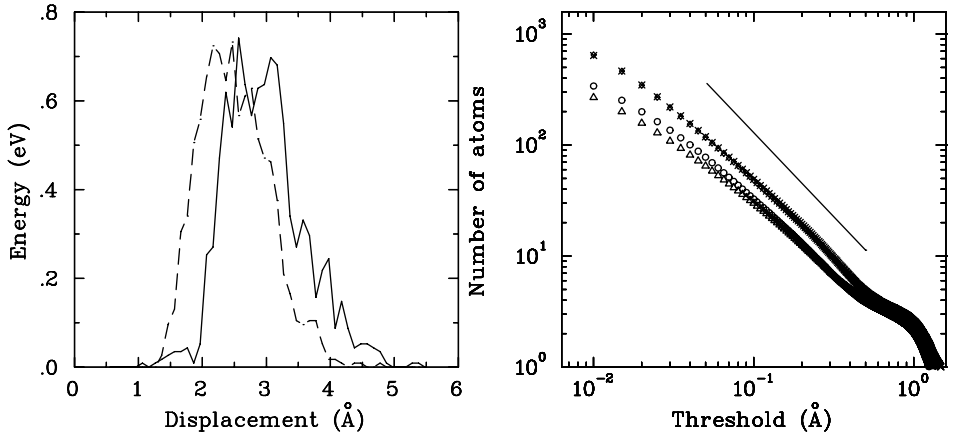

Figure 2: Left: Distribution of the square root of the sum of the squared atomic displacements between the initial and final configuration. Right: Number of atoms that have moved more than a distance r_c, plotted as a function of r_c.

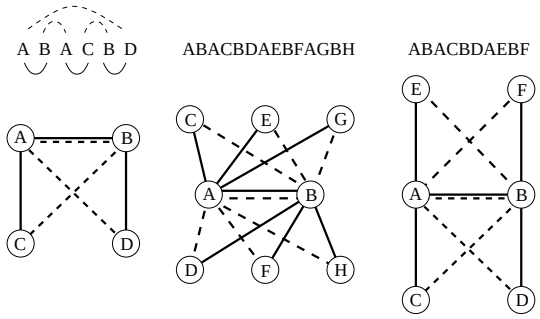

Figure 3: Most frequent events generated during the ART simulation. The left figure corresponds to the WWW bond-switching mechanism, the middle figure to concerted exchange, the right figure to a double bond-switching mechanism.

transpositions with the same shared bond. It is therefore not surprising that the third most common mechanism is a double bond-switching mechanism, see Fig. 3c. Here, the activation energy ranges from 3.5 eV to 17 eV. Clearly, this event is also energetically less favorable than single bond transpositions. Constructing the minimum-energy path of a subset of these events, Song and Mousseau found that this effect was increased with single WWW moves representing 90% of the relaxed events, and about 4 percent each of the CE and double WWW moves. Moreover, all of the CE and double WWW events had energy barriers higher than 4.5 eV [15].

The conclusion from this ART survey is that, in the absence of coordination defects, the dynamics of *a*-Si occurs predominantly through a sequence of structural changes based on bond transpositions: a pair of bonded atoms A and B (with neighboring atoms C and D, respectively) exchange these neighboring atoms, so that bonds AC and BD are replaced by bonds AD and BC.

COARSE-GRAINED DYNAMICS

The identification of the bond transposition as the dominant mechanism for the dynamics in *a*-Si provides a justification for using this mechanism in preparing atomistic models. Instead of molecular dynamics, one can directly evolve the system from one local energy minimum to the next through bond transpositions, as first proposed by Wooten, Winer and Weaire [6, 7].

Within the WWW approach, an atomic configuration consists of the coordinates of all N atoms, together with a list of the $2N$ bonds between them. The energy of a configuration is obtained from the Keating potential [18]:

$$E = \frac{3}{16}\frac{\alpha}{d^2}\sum_{\langle ij\rangle}\left(\mathbf{r}_{ij}\cdot\mathbf{r}_{ij} - d^2\right)^2 + \frac{3}{8}\frac{\beta}{d^2}\sum_{\langle jik\rangle}\left(\mathbf{r}_{ij}\cdot\mathbf{r}_{ik} + \frac{1}{3}d^2\right)^2. \quad (1)$$

Here, α and β are the bond-stretching and bond-bending force constants, respectively; $d = 2.35$ Å which is the equilibrium Si-Si bond length in the diamond structure. Usual values are $\alpha = 2.965\text{eV/Å}^2$ and $\beta = 0.285\ \alpha$.

Within this approach, the generation of a CRN starts with a cubic periodic diamond structure, which is then randomized by a large number of bond transpositions. After randomization, the network is relaxed through a sequence of many more proposed bond transpositions, accepted with the Metropolis acceptance probability:

$$P = \min\left[1, \exp\left(\frac{E_b - E_f}{k_b T}\right)\right], \quad (2)$$

where k_b is the Boltzmann constant, T the temperature, and E_b and E_f are the total *quenched* energies of the system before and after the proposed bond transposition.

With the approach described above, along with a few more details that can be found in Refs. [6, 7], Wooten, Winer and Weaire obtained 216-atom structures of *a*-Si with a bond angle deviation as low as 10.9 degrees. A decade later, using the same approach but more computing power, Djordjević, Thorpe and Wooten (DTW) produced larger (4096-atom) networks of even better quality; with a bond angle deviation of 11.02 degrees for configurations without four-membered rings and 10.51 degrees when these rings were allowed [19]. With some additional algorithmic improvements that we will discuss in the next paragraph, Barkema and Mousseau generated 1000-atom configurations with a bond angle deviation of 9.2 degrees [20], and one 4096-atom configuration with a bond angle deviation of 9.89 degrees. Elaborating on this work and exploiting parallel processing, Stijnman, Barkema and Bisseling obtained a 10000-atom sample with a bond-angle deviation as low as 9.84 degrees [21]. Besides a lower bond angle deviation, these samples also provide improved electronic properties (most notably a clean band gap in the electronic density of states).

The major improvements made to the standard WWW-algorithm are the following [20]:

1. The original WWW approach starts with a crystalline configuration, which is then randomized by a large number of bond transpositions. If the randomization is not continued long enough, the starting point for the relaxation still contains remnants of the initial crystalline state. In general, it is impossible to exclude the existence of crystalline remnants with this approach. To avoid this problem, we begin with a truly random initial state, i.e. a configuration with all atoms placed at random locations inside a periodic box at the crystalline density.

Table 1: Energetic and structural properties of models relaxed with the Keating potential. The first two models, DTW$^{(1)}$ and DTW$^{(2)}$ are the models described in Ref. [19] and refer, respectively, to a model with and without four-membered rings. BM1 and BM2 are 1000-atom models prepared following our procedure described in the text while '4096' and '10000' are, respectively, a 4096-atom and 10000-atom model prepared in the same way. All three models are without four-membered rings. The ring statistics shown here include irreducible rings only; ρ_0 is based on $r_0 = 2.35$ Å.

	DTW$^{(1)}$	DTW$^{(2)}$	BM1	BM2	4096	10000
E (eV/atom)	0.336	0.367	0.267	0.264	0.304	0.300
ρ/ρ_0	1.000	1.000	1.043	1.040	1.051	1.061
$\langle r\rangle/r_0$	0.996	0.997	0.982	0.982	0.980	0.978
$\Delta r/r_0$ (%)	2.52	2.65	3.94	3.71	4.17	4.18
$\langle\theta\rangle$	109.24	109.25	109.30	109.27	109.28	109.25
$\Delta\theta$	10.51	11.02	9.21	9.20	9.89	9.98

2. In well-relaxed configurations, most attempted bond transpositions are rejected. We abort the iterative relaxation process at an early stage, when it becomes clear that the bond transposition will eventually be rejected.

3. Immediately after a bond transposition, only a small cluster of atoms in the sample experience a significant force. This cluster consists of the atoms directly involved in the bond transposition (marked 'A', 'B', 'C' and 'D' in Fig. 3a) and of nearby atoms; typically atoms within the fourth neighbor shell of the four atoms involved in the transposition. During the initial phase of the relaxation, it is therefore sufficient to calculate the force *locally* (i.e. only for atoms inside the cluster) rather than *globally* (i.e. for all atoms in the sample). Most of the force evaluations are therefore of $\mathcal{O}(1)$, increasing significantly the efficiency of the algorithm for large models.

4. At regular intervals, we perform a full relaxation at T=0, trying systematically *all* possible moves until none can lead to a lower energy.

RESULTING CONFIGURATIONS

Using the algorithm described above, we have generated four different configurations: two 1000-atom cells (BM1 and BM2), one with 4096 atoms and one with 10000 atoms. A comparison of our models to the best such models generated before (those of Djordjević, Thorpe and Wooten [19]) is presented in Table 1. The strain per atom in our structures is significantly below that of DTW.

One of the standard measurements to evaluate the quality of a CRN is the coordination number of the atoms (the number of nearest neighbors). Using the minimum of the RDF between the first- and second- neighbor peak as the nearest neighbor cut-off distance and after relaxation with the Keating potential, the first two configurations are perfectly tetravalent. For the 4096-atom configuration, 0.1% of the atoms atoms are 5-fold coordinated; for the 10000-atom configuration, 0.02% and 0.14% of the atoms are 3-fold and 5-fold coordinated, respectively.

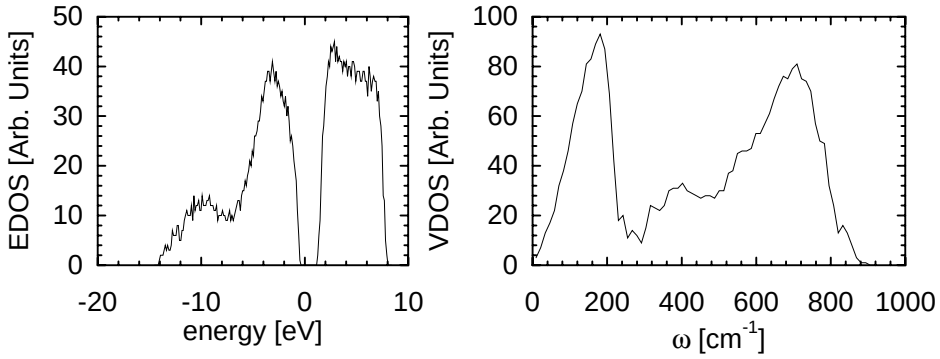

Figure 4: Left: The electronic density of states of configuration BM1; The band gap in the figure is estimated to be 1.5 eV. Right: The vibrational density of states of the same configuration obtained by calculating electronic forces using an $\mathcal{O}(1)$ algorithm.

The width of the bond angle distribution $\Delta\theta$ is another important measure for the quality of *a*-Si networks. This quantity can be determined experimentally from the RDF or from the Raman spectrum. In the latter case, a relation proposed by Beeman *et al.* [22], but with updated parameters as described in Ref. [23], has to be used. Recent experiments based on RDF measurements yield a bond angle deviation of 10.45 degrees for as-implanted *a*-Si and 9.63 degrees for annealed *a*-Si [24]. Our best configurations, relaxed with the Keating potential, display a bond angle deviation slightly below these experimental values. This is to be expected, however, since our models were prepared at zero K.

The main reasons for the large interest in *a*-Si are its electronic properties. It is therefore important to make sure that the electronic properties of our models are also good. These properties also provide indirect information about the structure: small densities of highly strained geometries (such as four silicon atoms forming a ring) or 3-fold coordination defects will be picked up as states in the gap of the electronic density of states (EDOS).

In Figs. 4(a) and 4(b) we have presented the electronic and vibrational density of states respectively for the configuration BM1 calculated within the framework of tight-binding approach. The tight-binding parameters for a-Si suggested by Kwon *et. al* [25] have been used to construct the Hamiltonian matrix elements. For the calculation of the vibrational density of states the dynamical matrix has been calculated numerically in the harmonic approximation by evaluating the electronic forces using an $\mathcal{O}(1)$ algorithm [26] which exploits the short-ranged nature of the density matrix.

In the last few years, it has become possible to compute the electronic structure of multi-thousand-atom configurations. In Fig. 5, we show the EDOS for the 10000-atom configuration.

Although we obtain good structures using the Keating potential, it is important to verify the stability of these networks when relaxed with a more realistic interaction potential that does not require a pre-set list of neighbors. The empirical potential that we use for this purpose is the Stillinger-Weber potential but with parameters optimized for *a*-Si. The parameters in the original SW potential were fitted to the liquid and crystalline phases of silicon; a refitting of the parameters to the amorphous phase is necessary to accurately describe that phase [27].

After relaxation with the modified SW potential, the two 1000-atom configurations remain perfectly four-fold coordinated. The 4096-atom and 10000-atom cells are less well relaxed and develop a small density of coordination defects. Based on the first minimum in the RDF, the 4096-

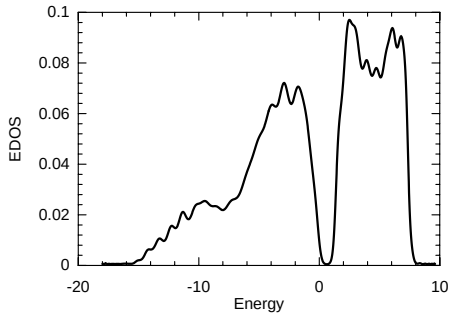

Figure 5: The electronic density of states of the 10 000-atom configuration, obtained with the tight-bnding interaction of Kwon *et al.*[25] combined with a maximum entropy approach to the EDOS [31].

atom sample displays, respectively, 0.4% and 0.3% of three-fold and five-fold coordinated atoms; for the 10000-atom sample these percentages are 0.3% and 0.3%, respectively.

Table 2 presents the structural and energetic properties of the relaxed networks at zero pressure. For all configurations, the bond angle distribution widens and the density decreases significantly compared to the Keating-relaxed structures. For the 1000-atom configurations, the local relaxation with the modified Stillinger-Weber potential did not result in a change of topology and the total energies are low compared with previous models [4]. We therefore expect the structures to be stable with any reasonable potential.

In Fig. 6 the RDF of one of our 1000-atom cells is plotted on top of experimental data obtained by Laaziri *et al.* [16] on annealed *a*-Si samples prepared by ion bombardment. The agreement is excellent, except for some discrepancy in the height of the third-neighbor peak. Agreement of the RDF should be taken as a minimum requirement of any reasonable sample configuration, not as a measurement of the quality of our cells; virtually all model configurations of *a*-Si show an RDF in agreement with experiment, and in fact even model configurations of some other materials like *a*-GaAs [29, 30].

SUMMARY AND OUTLOOK

Using the activation-relaxation technique, we have generated a database of more than 8000 atomistic activated events responsible for the relaxation and diffusion dynamics of amorphous silicon. From this database, we find hundreds of different mechansims which depend on the fine details of the local structure of the amorphous network. Most of the topological rearrangements, however, can be seen as variations on the bond-switching procedure proposed by Wooten, Winer and Weaire. This might explain why the WWW procedure remains, to this day, the best algorithm for generating high quality tetrahedral continuous random networks.

In view of these results, we have revisited the WWW algorithm and introduced a number of improvements that increased its efficienty by more than 2 orders of magnitude. The structural properties of the networks produced with this improved algorithm are excellent and they compare favorably to experiment. Moreover, the electronic density of states, obtained using tight-binding interactions [25] shows, for the first time in a numerical model, a wide and totally clean electronic

Table 2: Structural properties of our configurations after relaxation with the modified Stillinger-Weber (mSW) potential. The topology of the networks has not changed, except for the 4096-atom configuration (see text). For comparison, the total ring number per atom (including reducible rings) is also reported, as well as the energy after relaxation with the original Stillinger-Weber (SW) potential. MD-prepared configurations yield $E = -4.088$ eV/atom [28].

	BM1	BM2	4096	10000
E (eV/atom) (mSW)	-4.026	-4.034	-3.990	-3.994
E (eV/atom) (SW)	-4.126	-4.133	-4.106	-4.110
ρ/ρ_0	0.947	0.950	0.936	0.938
$\langle r \rangle / r_0$	1.018	1.017	1.020	1.020
$\Delta r / r_0$ (%)	2.9	2.7	3.2	3.1
$\langle \theta \rangle$	109.25	109.24	109.20	109.21
$\Delta\theta$	9.77	9.70	10.51	10.45
Rings/atom				
4	0.000	0.000	0.001	0.001
5	0.472	0.480	0.489	0.480
6	0.840	0.847	0.830	0.840
7	1.011	1.023	0.979	1.023
8	2.025	2.002	2.064	2.016

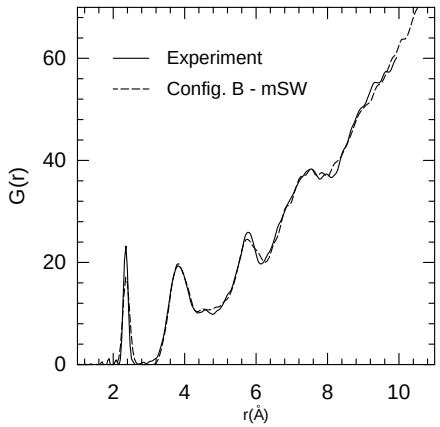

Figure 6: Radial distribution function for configuration BM2 relaxed with the modified Stillinger-Weber potential. Solid line: experimental results from Ref. [24].

band gap. Work on the application of parallel processing is in progress [21] to extend the sizes of the atomic models hopefully up to 10^5 atoms.

These high-quality models allow us to study more realistic problems involving hydrogen and dopants such as boron and phosphorus with a longer term goal of describing devices such as solar cells. At this point, for example, using periodic-boundary conditions in the two extended directions, we are be able to simulate *a*-Si films with thickness of about 1000 Å (about 400 atomic layers of 100 atom each, for a total of 40 000 atoms). Once such atomic configurations of a solar cell are available, the role of various structural and electronic defects can be studied.

ACKNOWLEDGEMENTS

We thank David Drabold for communicating to us the EDOS of our 10 000-atom sample. NM acknowledges partial support by the National Science Foundation under grant number DMR-9805848.

References

[1] T. A. Weber and F. H. Stillinger, Phys. Rev. B **32**, 5402 (1985).

[2] G. Boisvert, L. J. Lewis, and A. Yelon, Phys. Rev. Lett. **75**, 469 (1995).

[3] G. T. Barkema and N. Mousseau, Phys. Rev. Lett. **77**, 4358 (1996).

[4] N. Mousseau and G. T. Barkema, Phys. Rev. E **57**, 2419 (1998).

[5] N. Mousseau and G. T. Barkema, Phys. Rev. B (2000).

[6] F. Wooten, K. Winer, and D. Weaire, Phys. Rev. Lett. **54**, 1392 (1985).

[7] F. Wooten and D. Weaire, Solid State Physics **40**, 1 (1987).

[8] W. Frank, U. Gösele, H. Mehrer, and A. Seeger, in *Diffusion in Crystalline Solids*, edited by G. Murch and A. Nowick (Academic Press, New York, 1984).

[9] S. Roorda, W. C. Sinke, J. M. Poate, D. C. Jacobson, S. Dierker, B. S. Dennis, D. J. Eaglesham, F. Spaepen, and P. Fuoss, Phys. Rev. B **44**, 3702 (1991).

[10] J. H. Shin and H. A. Atwater, Phys. Rev. B **48**, 5964 (1993).

[11] G. Müller, G. Krötz, S. Kalbitze, and G. N. Greaves, Phil. Mag. B **69**, 177 (1994).

[12] R. Malek and N. Mousseau, Phys. Rev. E **62**, 7723 (2000).

[13] G. Mills and H. Jónsson, Phys. Rev. Lett. **72**, 1124 (1994).

[14] H. Jónsson, G. Mills and K.W. Jacobsen, "*Nudged Elastic Band Method for Finding Minimum Energy Paths of Transitions*" in "*Classical and Quantum Dynamics in Condensed Phase Simulations*", ed. B.J. Berne, G. Ciccotti and D.F. Coker (World Scientific, 1998).

[15] Y. Song and N. Mousseau, Phys. Rev. B **62**, 15680 (2000).

[16] K. Laaziri, S. Kycia, S. Roorda, M. Chicoine, J. L. Robertson, J. Wang, and S. C. Moss, Phys. Rev. Lett. **82**, 3460 (1999a).

[17] K. C. Pandey, Phys. Rev. Lett. **57**, 2287 (1986).

[18] P. N. Keating, Phys. Rev. **145**, 637 (1966).

[19] B. R. Djordjević, M. F. Thorpe, and F. Wooten, Phys. Rev. B **52**, 5685 (1995).

[20] G. T. Barkema and N. Mousseau, Phys. Rev. B **62**, 4985 (2000).

[21] X. Stijnman, G. T. Barkema, and R. Bisseling, *work in progress* (2001).

[22] D. Beeman, R. Tsu, and M. F. Thorpe, Phys. Rev. B **32**, 874 (1985).

[23] R. L. C. Vink, G. T. Barkema, and W. F. van der Weg, Phys. Rev. B **63**, 115210 (2001a).

[24] K. Laaziri, S. Kycia, S. Roorda, M. Chicoine, J. L. Robertson, J. Wang, and S. C. Moss, Phys. Rev. B **60** (1999b).

[25] I. Kwon, R. Biswas, C. Z. Wang, K. M. Ho and C. M. Soukoulis, Phys. Rev. B **49**, 7242 (1994).

[26] Parthapratim Biswas and G. T. Barkema, to be published.

[27] R. L. C. Vink, G. T. Barkema, W. F. van der weg, and N. Mousseau, J. Non-Cryst. Solids (2001b).

[28] L. J. Lewis and R. M. Nieminen, Phys. Rev. B **54**, 1459 (1996).

[29] N. Mousseau and L. J. Lewis, Phys. Rev. Lett. **78**, 1484 (1997a).

[30] N. Mousseau and L. J. Lewis, Phys. Rev. B **56**, 9461 (1997b).

[31] O. F. Sankey, and D. A. Drabold, Phys. Rev. Lett. **70**, 3631 (1993).